Title
Thermodynamics of Combustion in an Enclosure

Authors
Oppenheim, A.K.
Maxson, J.A.

Publication Date
1990-07-19

LBL-30890

Lawrence Berkeley Laboratory
UNIVERSITY OF CALIFORNIA

APPLIED SCIENCE
DIVISION

To be presented at the 13th International Colloquium on
Dynamics of Explosions and Reactive Systems,
Nagoya, Japan, July 28–August 3, 1991, and
to be published in the Proceedings

Thermodynamics of Combustion in an Enclosure

A.K. Oppenheim and J.A. Maxson

June 1991

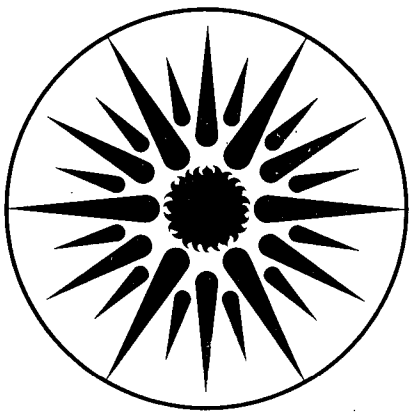

APPLIED SCIENCE
DIVISION

Prepared for the U.S. Department of Energy under Contract Number DE-AC03-76SF00098

DISCLAIMER

LBL-30890

Thermodynamics of Combustion in an Enclosure

A.K. Oppenheim and J.A. Maxson

Applied Science Division
Lawrence Berkeley Laboratory
University of California
Berkeley, California 94720

June 1991

This work was supported by the Director, Office of Energy Research, Office of Basic Energy Sciences, Engineering and Geosciences Division, and the Office of Industrial Processes, Advanced Industrial Concepts Division, of the U.S. Department of Energy under Contract No. DE-AC03-76SF00098, and by the U.S. Army Research Office under Contract No. DAAL03-87-K-0123.

Thermodynamics of Combustion in an Enclosure

A. K. Oppenheim and J. A. Maxson+*
University of California, Berkeley

Abstract

A systematically construed thermodynamic analysis of combustion in an enclosure is presented. The system is treated as one consisting of two components: the reactants and the products, both under the same, time varying, pressure. Whereas the former undergoes a prescribed change of state, usually isentropic or polytropic, the latter is, as a rule, at a thermodynamic equilibrium. In the course of the process, the two delineate distinct loci of states on a Le Chatelier diagram, trajectories on the plane of specific internal energy and the product of pressure and specific volume as its coordinates. The analysis is concerned then primarily with the evaluation of the consequences of three conditions of constraint: the balance of mass, balance of volume, and balance of energy, each forming a component of a vector equation. The application of this method of approach is illustrated by a number of examples. Its major advantage is the precision one gains in evaluating the relationship between pressure and mass, as well as volume, of the two components of the system.

Introduction

Combustion in a chamber under controlled conditions of material and energy fluxes is, for obvious reasons, of central importance to its technology. In the particular case of a closed vessel, it occupied thus a good deal of attention in the literature, its salient features having been treated at some length in most reference books on combustion, including prominently the classical monographs of Lewis and von Elbe [1] and Zeldovich et al. [2], as well, of course, as in all the texts of particular relevance to internal combustion engines [3-8]. Concomitantly, its treatment has been included, as a matter of course, in all the computational algorithms for internal combustion engines (e.g. [9-14]) as well as in a great number of papers on this subject (e.g. [15-23]).

Introduced here is a comprehensive approach to the subject following a somewhat different method of attack than usual. Its major attributes are straightforwardness, simplicity, and convenience, as well as particular

---

*Professor of Engineering
+Research Assistant

suitability to numerical computations and, last but by no means least, applicability to any combustion system, irrespectively whether the process is accomplished by a distinct flame front traversing the reactants or whether it occurs in a highly turbulent flow field, such as that of a pulsed jet plume currently under study. By the same token our analysis is completely independent of the normal burning speed, a parameter introduced usually right from the outset.

The salient feature of our method of approach is the adoption of the product of pressure and specific volume, the difference between enthalpy and internal energy, w, as the principal thermodynamic reference parameter, whereas the loci of states of the two components are delineated on the appropriate Le Chatelier diagram, the plane of specific internal energy and w. The analysis is concerned then with the evaluation of the consequences of three conditions of constraint: the balance of mass, balance of volume, and balance of energy. The implementation of this method is illustrated by a number of examples demonstrating that its most significant advantage is the precision it provides for the evaluation of the relationship between pressure and mass, as well as volume, of the two components of the system, including in particular global effects of heat transfer to surroundings.

Method

Consider a combustion system in an enclosure separating the reacting medium from the surroundings. In general, the motion of the walls, as well as a certain amount of mass and heat transfer across them, may be taken into account, provided that these phenomena are specified in terms of the displacement rate and fluxes, and that their influence is not too extensive to destroy the identity of the system. Under normal conditions we wish to consider here, the molecular diffusivity of the reacting medium is definitely less than 10 cm^2/sec, while the representative length of the enclosure is not much less than 10 cm. The effective time for diffusion to affect the system is then at least 10 sec, whereas the time interval of the process of combustion under study is measured, at most, in tens of milliseconds - a practically thousandfold difference in characteristic times.

Under such circumstances one deals, in effect, with a two-component system, one consisting of the reactants, R, and products, P, confined within an enclosure, Σ, wherein the process of combustion is governed by three thermodynamic conditions of constraint: the balances of mass, M, volume, V, and energy, E.

Our method of approach is associated with the adoption of the variable

$$w_K \equiv pv_K = \frac{\Re T_K}{M_K} \qquad (1)$$

where K ≡ R, P#, as the principal thermodynamic reference parameter. This follows in fact the methodology introduced by the senior author for the analysis of processes associated with the action of gasdynamic discontinuities in explosive media [24]. The applicability of the above equation is, of course, subject to condition that all the constituents of gaseous products obey the

---

#symbols defined in the Nomenclature.

perfect gas equation of state, whereas the contribution of condensed phase to the total volume is practically negligible. In internal combustion engines this is usually the case, as, indeed, recognized in all the references cited here.

Noting also that the thermodynamic pressure in such a system is spatially uniform, being solely a function of time, i.e.

$$p_R = p_P = p_\Sigma = p(t) \tag{2}$$

the three conditions of constraint can be expressed simply in terms of a vector equation

$$R + P = \Sigma \tag{3}$$

where, with K ≡ R, P,

$$K = \begin{Bmatrix} M_K \\ w_K M_K \\ u_K M_K \end{Bmatrix} \tag{4}$$

are the vectors of the reactants and products, whereas

$$\Sigma = \begin{Bmatrix} M_\Sigma \\ pV_\Sigma \\ E_\Sigma \end{Bmatrix} \tag{5}$$

is the vector of the enclosure, its components being specified by the wall conditions. As apparent from eq. (5), the second components of these vectors express the volume balance multiplied by p.

The most appropriate thermodynamic plane for our analysis is that of u vs w, a refined version of the so-called Le Chatelier diagram. As a consequence of the definition of enthalpy, this diagram has a number of interesting properties:

1. The shift from the locus of states of the reactants to that of the products at constant w is a measure of the specific exothermic energy, i.e.

$$q_w = (u_R - u_P)_w \equiv (h_R - h_P)_w \tag{6}$$

2. In terms of the slope $c_K = du_K/dw_K$, the isentropic index

$$\Gamma \equiv -\left(\frac{\partial \ln p}{\partial \ln v}\right)_s = \left(\frac{\partial h}{\partial u}\right)_s = (c_K + 1)/c_K$$

whence

$$\left(\frac{\partial \ln p}{\partial \ln w}\right)_s = c_K + 1 \tag{7}$$

providing a direct relation between p and w, whenever the locus of states is tangent to an isentrope.

3. The locus of h = const. is a straight line inclined at a slope $(\partial u/\partial w)_h = -1$.

4. The functional relationship u = u(w) is fully equivalent to h = h(w).

The formulation of the problem is closed by postulating the changes of states for the two components of the system. The reactants are usually assumed to undergo an isentropic process, or, in engineering applications, one obeying a polytropic law, while the products are, as a rule, at a thermodynamic equilibrium. The implementation of the method is illustrated by examples in the following section. All the equilibrium computations required for this purpose have been carried out using STANJAN (25), a most convenient code devised by Reynolds at Stanford that is heartily recommended to anyone interested in the subject.

Implementation

Isolated Enclosure

For an isolated system, the vector of the enclosure is specified in terms of three invariants: $M_\Sigma = M_i$, $V_\Sigma = V_i$, and $E_\Sigma = E_i$, where subscript i denotes initial conditions.

Eliminating mass from eqs. (3), with (4) and (5), one obtains then

$$u_P = aw_P + b \qquad (8)$$

where

$$a = (u_R - u_i) / (w_R - pv_i)$$
$$b = (u_i w_R - pv_i u_R) / (w_R - pv_i)$$

a linear relation for a fixed point on R at a given p. The concomitant point on P is then determined by the intersection of the straight line thus specified with the corresponding locus of equilibrium states at constant pressure.

An example of a Le Chatelier diagram, constructed in this fashion for a particular case of a propane-air mixture at an equivalence ratio $\phi = 0.6$ for initial pressure of 5 atm and a temperature of 60°C, is presented in Fig. 1. Loci of the reactants, assumed to undergo an isentropic process, and of products, delineating states of thermodynamic equilibrium, are displayed by thick lines, while thin lines are plots of eq. (8) indicating corresponding points at the same pressures.

The variation of all the thermodynamic parameters with respect to, in turn, product mass fractions, μ_P and volume fractions, η_P are depicted, respectively, on Fig. 2 and 3. It is of interest to note that, on the former, pressure plots as a practically straight line, in accord with a widely accepted practical rule that pressure in a closed container is with good approximation proportional to the product mass fraction. Fundamental reasons for this rule are presented here later as a consequence of the linear approximation.

Layered Combustion

Of central interest to the history of the subject is the case of the so-called layered combustion. Its theory, founded by Flamm and Mache [26] in 1917, has been used as the basis for evaluating laminar burning speeds from measurements made in closed spherical vessels with combustion initiated at the center. According to it in the course of the process the reactants, as well as the products, are compressed isentropically, while the

transition between them takes place as a jump at constant enthalpy. The monotonic temperature rise of the products obtained thereby layer by layer as the reactants traverse the flame front has been referred to as the *Mache effect* in practically all the publications on this subject.

The Le Chatelier diagram, for the same chemical system and initial conditions as before, is shown in Fig. 4. Loci of states for the reactants and products are now isentropes at frozen composition, but, whereas this is uniformly so for the reactants, the initial composition of products is different for each elementary process. Initially, for example, there is a transition from i on R to hp on P, followed by isentropic compression to the final pressure at i on P. Then, as exemplified by the intermediate processes, an isentropic compression of reactants up to points 1 or 2 on R is followed by a constant enthalpy transition to P and succeeded by an isentropic compression up to points 1 and 2 on P. Finally, upon an isentropic compression of reactants to point f on R, there is just the transition at constant enthalpy and pressure to point f on P. The temperature profiles thus determined are shown on Fig. 5 and 6, plotted as a function of, respectively, product mass and volume fractions. Displayed there by chain-broken lines are the corresponding temperatures computed for the previous case. The latter is in excellent agreement with the mass averaged temperature, as evident in Fig. 5, whereas it differs significantly from the volume averaged temperature, as apparent in Fig. 6.

Linear Approximation

The straight-line appearance of the loci of states on the Le Chatelier diagram suggest the accuracy and, hence, usefulness of linear approximation based on the postulate that

$$c_K \equiv (\partial u/\partial w)_K = const.$$

The recipe for its application is then as follows:

1. With respect to the initial point, i, on R, determine the points hp and uv on P, corresponding, respectively, to the enthalpy and pressure, and to the internal energy and volume, of state i; whence one gets the slope c_P of the locus of products.

2. Evaluate the final point, f, on R as the end state of a frozen isentropic process from state i, corresponding to the pressure of state uv on P, specifying thus the slope c_R of the locus of reactants.

3. Calculate the reference exothermic energy as the distance between the intersection of the straight lines thus delineated and the w = 0 axis, i.e.

$$q = c_P w_{uv} - c_R w_i \qquad (9)$$

In reducing the formulae to a non-dimensional form, the scale for u is shifted, as it can be without any restriction, so that

$$\left.\begin{aligned} u_R &= c_R w_R \\ u_P &= c_P w_P - q \end{aligned}\right\} \qquad (10)$$

Thus, in terms of parameters normalized with respect to initial conditions, $\mu_K \equiv M_K/M_i$, $W_K \equiv w_K/w_i$, and $Q \equiv q/c_R w_i$, where $K \equiv R, P, uv$, while $k \equiv c_P/c_R$, one has

$$Q = kW_{uv} - 1 \qquad (9')$$

$$\left.\begin{aligned} U_R &= W_R \\ U_P &= kW_P - Q \end{aligned}\right\} \qquad (10')$$

so that, with $P \equiv p/p_i$, the vectors of eq. (3) are now:

$$R = \begin{Bmatrix} \mu_R \\ W_R\mu_R \\ W_R\mu_R \end{Bmatrix} \; ; \; P = \begin{Bmatrix} \mu_P \\ W_P\mu_P \\ (kW_P - Q)\,\mu_P \end{Bmatrix} \; ; \; \Sigma = \begin{Bmatrix} 1 \\ P \\ 1-\epsilon_\lambda \end{Bmatrix} \qquad (11)$$

where $\epsilon_\lambda \equiv E_\lambda/E_i$ is the normalized heat loss term.

For example, according to our recipe, the data of Fig. 1 yield $c_P = 3.88$, $c_R = 2.77$ and $q = 2$ kJ/g, whence $k = 1.395$ and $Q = 7.85$.

From the mass and volume balances of eqs. (3) and (11), it follows that

$$W_P = [P - (1 - \mu_P)\,W_R]\,/\,\mu_P \qquad (12)$$

while from the volume and energy balance one obtains

$$\mu_P = [P - 1 + \epsilon_\lambda]\,/\,[Q - (k - 1)\,W_P] \qquad (13)$$

whence, eliminating W_P,

$$\mu_P = [kP - 1 - (k-1)\,W_R + \epsilon_\lambda]\,/\,[Q - (k-1)\,W_R] \qquad (14)$$

If, moreover, as is often the case, it is assumed that the reactants are compressed isentropically,

$$P = W_R^{\sigma_R + 1} \qquad (15)$$

- a direct consequence of eq. (7).

Equations (14) and (15) specify the product mass fraction, μ_P, for a given state of reactants identified by its pressure, P. This is the key to the solution, for, once this relationship is established, all the thermodynamic parameters and, hence, the volume fractions, can be evaluated simply as follows:

$$\tau_R \equiv T_R/T_i = W_R = P^{\,1/(\sigma_R + 1)} \qquad (16)$$

$$v_R \equiv v_R/v_i = W_R/P = P^{\,-\sigma_R/(\sigma_R + 1)} \qquad (17)$$

$$\eta_R \equiv V_R/V_i = \mu_R v_R = (1-\mu_P)\,P^{\,-\sigma_R/(\sigma_R + 1)} \qquad (18)$$

while, in terms of W_P specified by eq. (12),

$$\tau_P \equiv T_P/T_i = mW_P \qquad (19)$$

$$\nu_P \equiv v_P/v_1 = W_P/P \qquad (20)$$

$$\eta_P \equiv V_P/V_1 = 1 - \eta_R \qquad (21)$$

where $m \equiv M_P/M_R$ is evaluated by linear interpolation between m_{hp} and m_{uv}.

For an adiabatic enclosure, $\epsilon_\lambda = 0$. If, moreover, k = 1, eqs. (13) and (14) yield simply

$$\mu_P = (P - 1)/Q \qquad (22)$$

providing a proof of the well known rule of proportionality between the product mass fraction and the pressure rise. If k = 1, while $(k - 1)W_P << Q$, the functional relationship, $P = P(\mu)$ is still practically linear, as it appears in Fig. 2.

The results obtained this way are presented by points on Fig. 3. Their remarkable coincidence with the continuous curves obtained by detailed equilibrium computations provide a most satisfactory demonstration of the amazing accuracy of linear approximation for a dilute mixture.

In the non-adiabatic case, if one wishes to reduce the analysis to its simplest form, the heat loss term, ϵ_λ, has to be expressed in an integral form. One can thus obtain a reasonable estimate by assuming that it is proportional to the area of contact between the hot products and the walls, as well as to their temperature difference. Thus

$$\epsilon_\lambda = \lambda a(\tau_P - 1) = \lambda a(mW_P - 1) \qquad (23)$$

where $a \equiv A_P/A_\Sigma$.

In view of eq. (12), this can be written as

$$\epsilon_\lambda = \lambda a[m(P - W_R)/\mu_P + mW_R - 1] \qquad (24)$$

Under such circumstances eq. (14) provides a quadratic equation for $\mu_P = \mu(P,W_R)$ whose positive root, combined with eq. (15), yields an univalued function $\mu_P = \mu(P)$.

The proportionality factor, λ, is evaluated from eqs. (13) and (23) by noting that, at $\mu_P = 1$, $P = W_R = P_{max}$ (since then $\nu_P = 1$), while a = 1, so that

$$\lambda = (Q + 1 - kP_{max})/(mP_{max} - 1) \qquad (25)$$

The geometric factor can be related to the product volume fraction by postulating that

$$a = [\eta_P^{2/3} - (\eta_P^*)^{2/3}]/[1 - (\eta_P^*)^{2/3}] \qquad (26)$$

where the asterisk indicates the critical volume fraction burnt when the products first get in contact with the wall.

The concomitant critical product mass fraction, μ_{P*}, is estimated by assuming that it is proportional to P_{max}. The latter varies from the lower limit established empirically for the case of $\eta_P^* = \mu_P^* = 0$, realized for the FTC mode of combustion (the process initiated by a spark discharge in close

proximity of the wall), to the upper limit, corresponding to an isolated enclosure. For $\eta_P < \eta_P^*$ the process of combustion is, of course, adiabatic.

The results are presented in Figs. 7-13. Figure 7 depicts the Le Chatelier diagram for an enclosure of constant volume with heat losses, when the critical product volume fraction $\eta_P^* = 0.3$, while profiles of all the thermodynamic parameters with respect to the product mass and volume fractions are displayed in Figs. 8 and 9. For the latter $\lambda = 0.7$, a value obtained from eq. (25) for $P_{max} = 4.56$, established experimentally when, from concomitant schlieren records, $\eta_P^* = 0.3$. Figures 10 and 11 describe the pressure profiles as a function of the two fractions for an array of critical volume fractions, while the corresponding temperature profiles are shown in Figs. 12 and 13.

Conclusions

Presented here is a novel approach to an old problem. It reflects, in effect, the progress ushered in by the computational facilities available today for the evaluation of thermodynamic loci of states satisfying a specified set of constraints. A significant simplification is attained by adopting the pressure - specific volume product, w, as the thermodynamic reference coordinate.

On the basis of well established empirical evidence, one deals then with a system of two components: the reactants and the products, undergoing the process of combustion under the restriction of three thermodynamic conditions of constraint: the balances of mass, volume, and energy.

The shift between the two loci of states on the Le Chatelier diagram (a plot of internal energy, or enthalpy, as a function of w) at constant w specifies unambiguously the exothermic energy, referred to colloquially as the heat of combustion.

The method of approach is illustrated by a number of elementary examples where the conditions at the walls of the enclosure are expressed in terms of integral quantities, rather than rates of displacement or fluxes that describe usually the mass and energy transport across them.

The basic case is that of an isolated enclosure where the products are well mixed, the maximum entropy limit. This is contrasted to the case of layered combustion, displaying the so-called *Mache effect*, the minimum entropy limit where the products are completely unmixed.

In both cases the system under study undergoes a transition from a process at constant pressure to that at constant volume.

Taking advantage of the observation that the loci of states on the Le Chatelier diagram, using w as the reference coordinate, are effectively straight-linear, a *linear approximation* is introduced. Upon the demonstration of its accuracy, this approximation is then used to estimate the influence of heat losses at the walls upon the profiles of thermodynamic parameters with respect to product mass and volume fractions. The heat loss term has been for this purpose expressed by an integral relation.

It is on this basis that we have been able to achieve satisfactory precision in deducing the amount of products of the exothermic reaction in turbulent plumes of pulsed jets, recorded by schlieren photographs, from the concomitant pressure transducer records [27,28].

If the mass or energy transport across the walls is given in terms of the rates of displacement or fluxes, the thermodynamic conditions of constraint are expressed in terms of O.D.E.'s combined with algebraic equations. They

specify then the thermodynamic parameters which, in a computational scheme, are required for the evaluation of the flow field. The O.D.E.'s are then non-linear and autonomous, acquiring the form of equations of growth. The task of solving the problem becomes then equivalent to seeking the determination of integral curves (trajectories) on a phase plane, the plane of dependent variables of the same kind as Figs. 2, 3, 8 and 9. The background for this procedure and the results of modeling analyses of combustion in a piston-cylinder enclosure, based on it, have been presented elsewhere [29-32].

Acknowledgment

Work on this paper was supported by the Director, Office of Energy Research, Office of Basic Energy Science, Engineering and Geosciences Division, and the Office of Industrial Processes, Advanced Industrial Concepts Division of the U.S. Department of Energy, under Contract No. DE-AC03-76SF00098, and by the U.S. Army Research Office under Contract No. DAAL03-87-K-0123.

References

1. B. Lewis and G. von Elbe, *Combustion, Flames and Explosion of Gases*, (esp. Chapter V, *15. Combustion Waves in Closed Vessels*, pp. 381-395), Third Edition, xxiv + 739 pp., Academic Press, Inc., Orlando, Florida, 1987.
2. Ya. B. Zeldovich, G. I. Barenblatt, V. B. Librovich, and G. M. Makhviladze, *The Mathematical Theory of Combustion and Explosions*, 478 pp., 1980 (esp. Chapter 6, *2. Combustion in Closed Vessels, The Mache Effect*, pp. 470-487), transl. D. H. McNeill, Consultants Bureau, New York and London, xxi + 597 pp., 1985.
3. C. F. Taylor, *The Internal-Combustion in Theory and Practice, 1: Thermodynamics, Fluid Flow, Performance*, x + 574 pp., The MIT Press, Cambridge, Mass., 1985.
4. C. F. Taylor, *The Internal-Combustion Engine in Theory and Practice, 2: Combustion, Fuels, Materials, Design*, x + 783 pp., The MIT Press, Cambridge, Mass., 1982.
5. E. F. Obert, *Internal Combustion Engines and Air Pollution*, xiii + 740 pp., Harper & Row, Publishers, New York, 1973.
6. J. B. Heywood, *Internal Combustion Engine Fundamentals*, xxix + 930 pp., McGraw-Hill Book Company, New York, 1988.
7. R. S. Benson, (J. H. Horlock and D. E. Winterbone, Editors), *The Thermodynamics and Gas Dynamics of Internal Combustion Engines, 1*, xx + 580 pp., Clarendon Press, Oxford, 1982.
8. J. H. Horlock, and D. E. Winterbone Editors, *The Thermodynamics and Gas Dynamics of Internal-Combustion Engines, II*, (esp. Chapter 14. *Combustion and Cycle Calculations in Spark Ignition Engines* by P.C. Baruah, p. 823), xxxvi + 1237 pp., Clarendon Press, Oxford, 1982.
9. W. J. D. Annand, "A New Computation Model of Combustion in the Spark Ignition Engine," *Proc. I. Mech. E., 185*, 119-126, 1970.
10. G. G. Lucas, and E. H. James, "A Computer Simulation of a Spark Ignition Engine," SAE Paper No. 730053, 1973.
11. F. V. Bracco, "Introducing a New Concentration of More Detailed and Informative Combustion Models," SAE Paper No. 741174, 1974.

12. R. S. Benson, W. J. D. Annand, and P. C. Baruah, "A Simulation Model Including Intake and Exhaust Systems for a Single Cylinder Four-Stroke Cycle Spark Ignition Engine," *Int. J. Mech. Sci., 17*, 97-124, 1975.
13. K. Meintjes, *A User's Guide for the GM Engine Simulation Program*, GM Research Publication GMR-5788, II + 17 pp., 1987.
14. W. C. Reynolds, *Engine Simulation Program*, Department of Mechanical Engineering, Stanford University, Stanford, California, 8 pp., 1987.
15. R. B. Krieger, and G. L. Borman, "The Computation of Apparent Heat Release for Internal Combustion Engines," ASME Paper No. 66-WA/DGP-4, 1966.
16. G. A. Lavoie, J. B. Heywood, and J. C. Keck, "Experimental and Theoretical Study of Nitric Oxide Formation in Internal-Combustion Engines," *Combust. Sci. Tech., 1*, 313-326, 1970.
17. N. C. Blizard, and J. C. Keck, "Experimental and Theoretical Investigation of Turbulent Burning Model for Internal-Combustion Engines," SAE Paper No. 740191, 1974.
18. D. R. Lancaster, R. B. Krieger, S. C. Sorenson, and W. Hull, "Effects of Turbulence on Spark Ignition Engine Combustion," SAE Paper No. 760160, 1976.
19. R. J. Tabaczynski, C. R. Ferguson, and K. Radhakrishnan, "A Turbulent Entrainment Model for Spark Ignition Engine Combustion," SAE Paper No. 770647, 1977.
20. F. D. McCuiston, Jr., G. A. Lavoie, and C. W. Kauffman, "Validation of a Turbulent Flame Propagation Model for a Spark Ignition Engine," SAE Paper No. 770045, 1977.
21. G. I. Sivashinsky, "Hydrodynamic Theory of Flame Propagation in an Enclosed Volume," *Acta Astronautica, 6*, 631-645, 1979.
22. T. Takeno, and T. Iijima, "A Theoretical Analysis of Flame Propagation in Closed Vessels," *Trans. Japan Society for Aero. & Space Sciences, 28*, 79, 1-15, 1985.
23. Y. Tanaka, "Numerical Simulations for Combustion of Quiescent and Turbulent Mixtures in Confined Vessels," *Combustion and Flame, 75*, 123-138, 1989.
24. A. K. Oppenheim, *Introduction to Gasdynamics of Explosions*, Springer-Verlag, Wien-New York, VI + 220 pp., 1972.
25. W. C. Reynolds, *STANJAN Interactive Computer Programs for Chemical Equilibrium Analysis*, Department of Mechanical Engineering, Stanford University, Stanford, California, Version 3, 48 pp., 1986.
26. L. Flamm, and H. Mach, "Combustion of an Explosive Gas Mixture within a Closed Vessel," *Berichte, Wien Akad. Wissenschaften, 26*, 9ff., 1917.
27. A. K. Oppenheim, J. Beltramo, D. W. Faris, J. A. Maxson, K. Hom, and H. E. Stewart, "Combustion by Pulsed Jet Plumes - Key to Controlled Combustion Engines," SAE Paper No. 890153, 1989.
28. J. A. Maxson, and A. K. Oppenheim, "Pulsed Jet Combustion - key to a refinement of the stratified charge concept," *Twenty-Third Symposium (International) on Combustion*, Orleans, France, 1990.
29. A. K. Oppenheim, "The Beauty of Combustion Fields and Their Aerothermodynamic Significance," *Prog. in Astro. & Aero., 105*, 3-13, AIAA, Washington, D.C., 1986.
30. A. K. Oppenheim, and D. A. Rotman, "Fundamental Features of Ignition and Flame Propagation in Engines," ASME Paper No. 87-ICE-21, 8 pp., 1987.

31. D. A. Rotman, and A. K. Oppenheim, "Aerothermodynamic Properties of Stretched Flames in Enclosures," *Twenty-First Symposium (International) on Combustion*, 1303-1312, The Combustion Institute, Pittsburgh, Pa., 1986.
32. D. A. Rotman, M. Z. Pindera, and A. K. Oppenheim, "Fluid Mechanical Properties of Flames in Enclosures," *Progress in Astronautics and Aeronautics, 113*, 251-266, AIAA, Washington, D.C., 1988.

Nomenclature

Symbols

a	A_P/A_Σ
A	area of contact
c	slope of the locus of states on the Le Chatelier diagram
E	energy
h	specific enthalpy
m	M_P/M_R
M	mass
$\mathcal{M}$	molecular mass
p	pressure
P	products or p/p_i
q	specific exothermic energy
Q	$q/c_R w_R$
R	reactants
$\Re$	gas constant
s	entropy
t	time
T	temperature
u	specific internal energy
U	u/u_i
v	specific volume
V	volume
w	pv
Γ	isentropic index
ϵ	E/E_i
η	volume fraction
λ	heat loss factor
μ	mass fraction
ν	v/v_i
Σ	enclosure
τ	T/T_i
ϕ	equivalence ratio

Subscripts

f	final
i	initial
hp	state of products at $h = h_i$ and $p = p_i$
K	R,P
P	products
R	reactants
s	constant entropy

uv	**state of products at $u = u_i$ and $v = v_i$**
w	**constant w**
Σ	**enclosure**
λ	**lost**

Figures

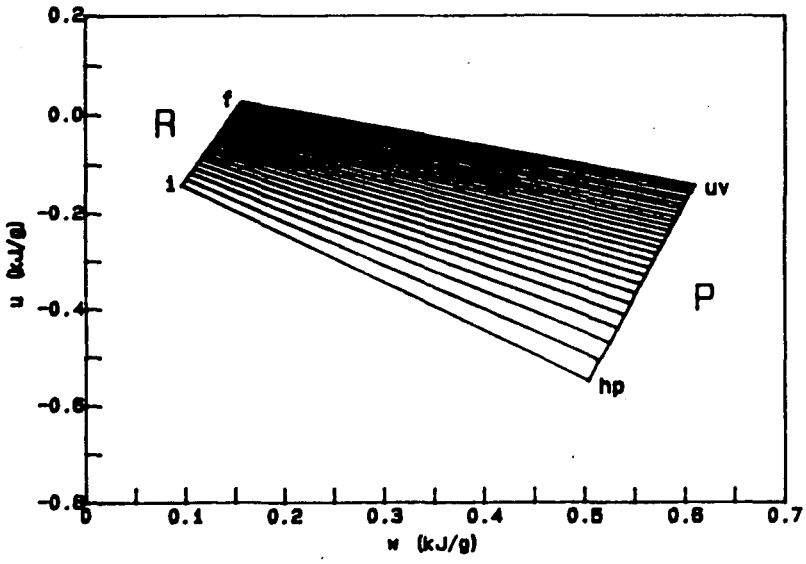

Fig. 1 The Le Chatelier diagram for an isolated enclosure

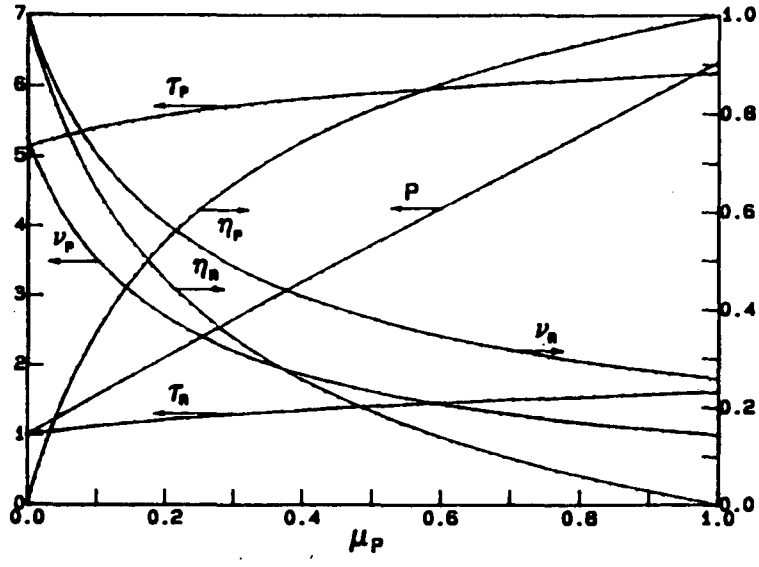

Fig. 2 Solution for an isolated enclosure as a function of product mass fraction

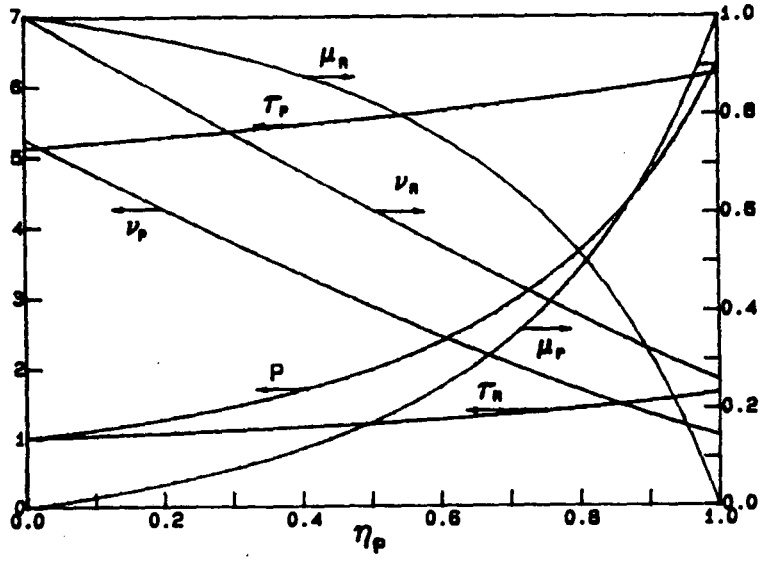

Fig. 3 Solution for an isolated enclosure as a function of product volume fraction

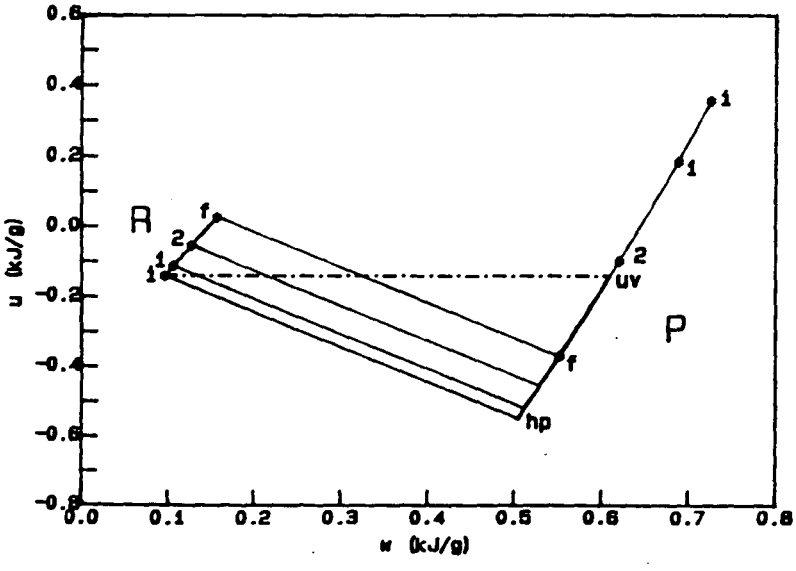

Fig. 4 The Le Chatelier diagram for layered combustion

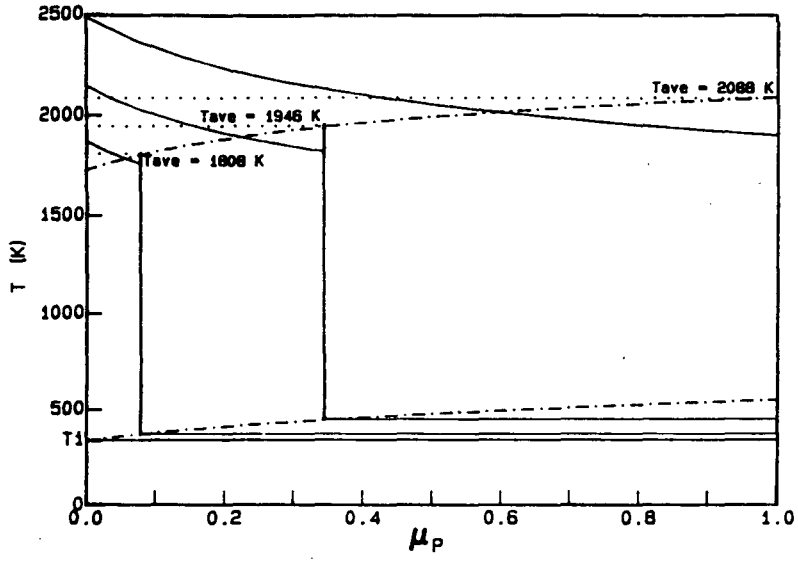

Fig. 5 Temperature profiles for layered combustion with respect to product mass fraction

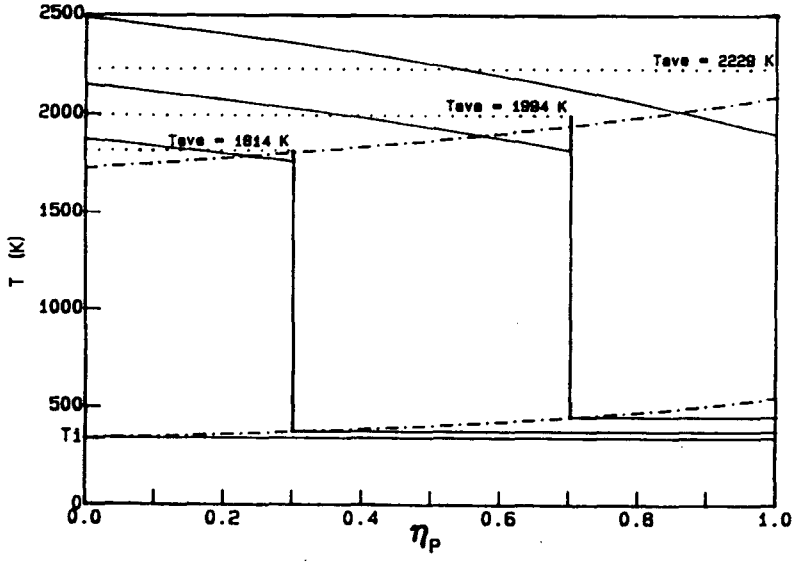

Fig. 6 Temperature profiles for layered combustion with respect to product volume fraction

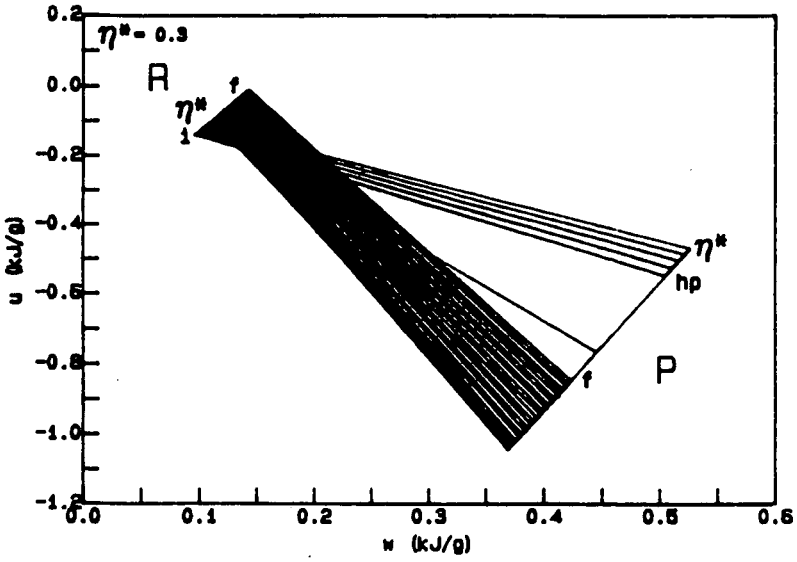

Fig. 7 The Le Chatelier diagram for an enclosure of constant volume with heat losses when the critical product volume fraction $\eta_P^* = 0.3$

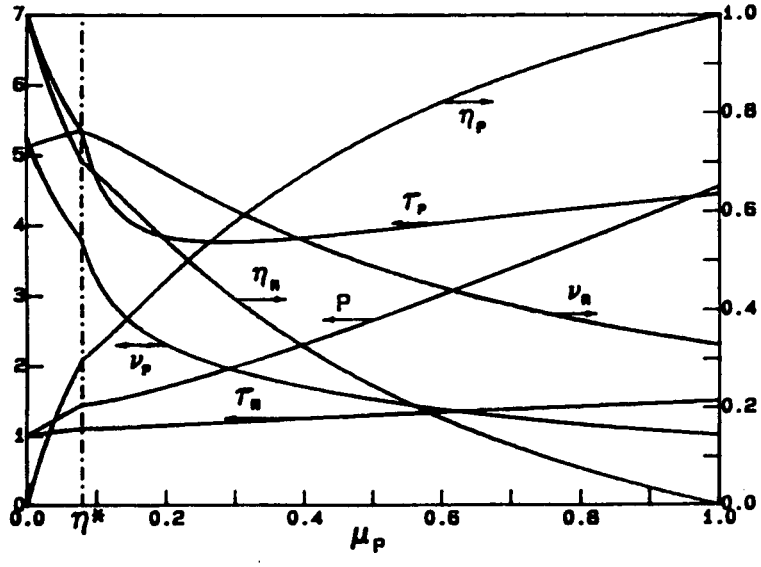

Fig. 8 Solution for an enclosure of constant volume with heat losses when the critical product volume fraction $\eta_P^* = 0.3$, as a function of product mass fraction

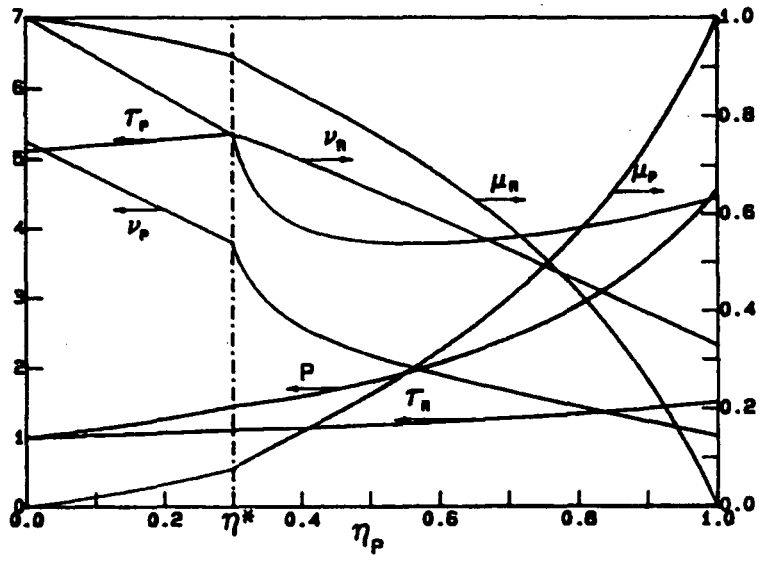

Fig. 9 Solution for an enclosure of constant volume with heat losses when the critical product volume fraction $\eta_P^* = 0.3$, as a function of product volume fraction

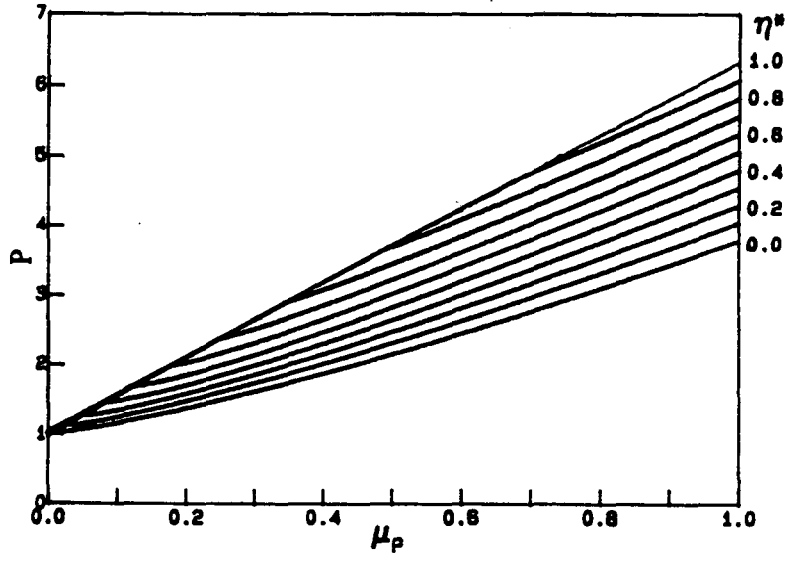

Fig. 10 Pressure profiles for an enclosure of constant volume with heat losses corresponding to an array of critical product volume fractions, η_P^*, with respect to product mass fraction

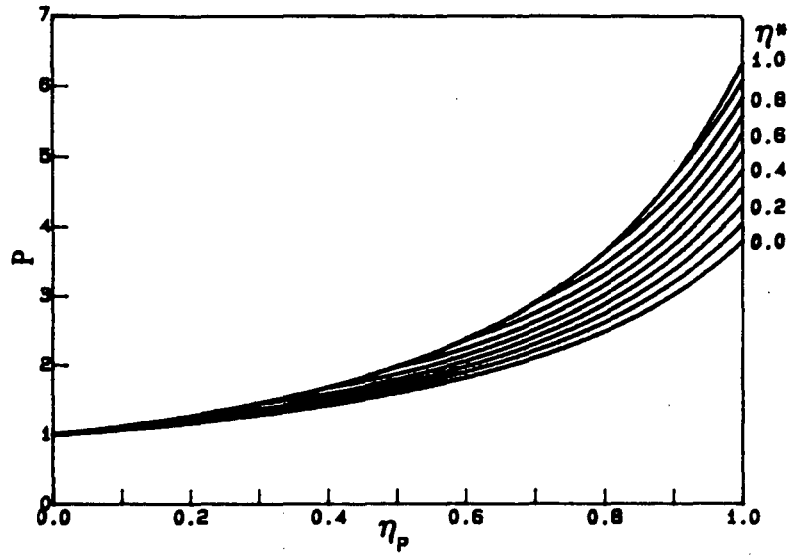

Fig. 11 Pressure profiles for an enclosure of constant volume with heat losses corresponding to an array of critical product volume fractions, η_P^*, with respect to product volume fraction

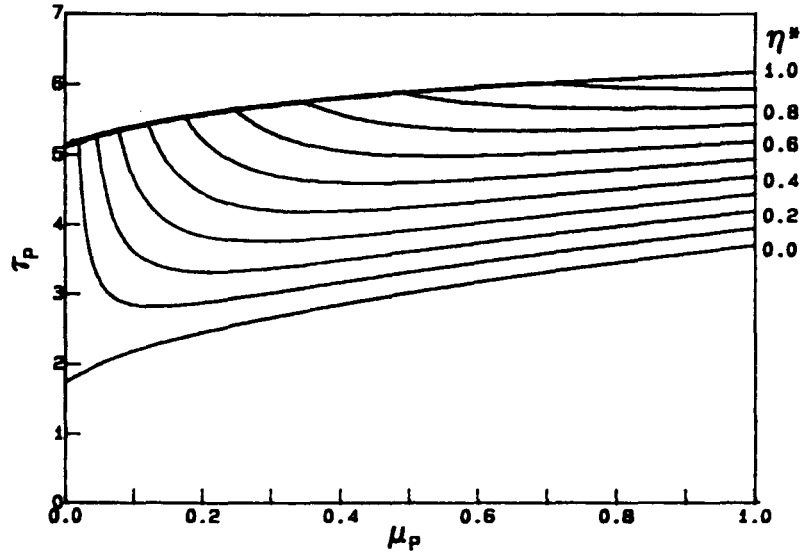

Fig. 12 Temperature profiles for an enclosure of constant volume with heat losses corresponding to an array of critical product volume fractions, η_P^*, with respect to product mass fraction

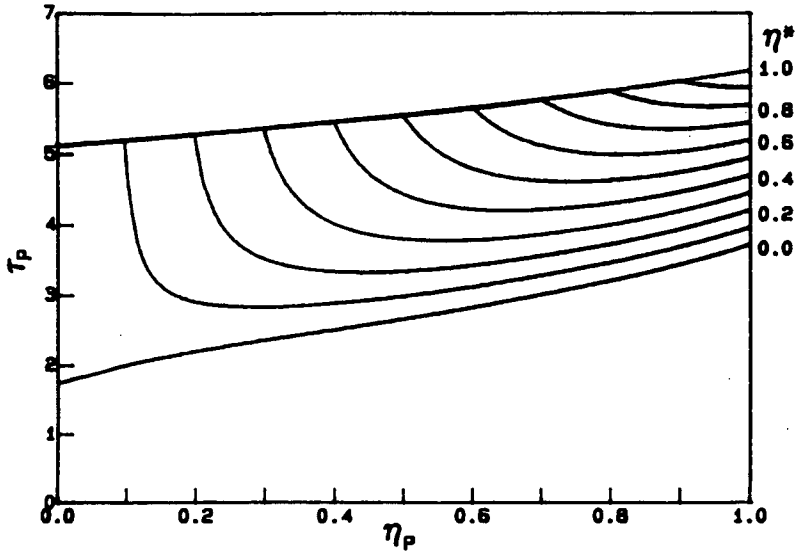

Fig. 13 Temperature profiles for an enclosure of constant volume with heat losses corresponding to an array of critical product volume fractions, η_p^*, with respect to product volume fraction

LAWRENCE BERKELEY LABORATORY
UNIVERSITY OF CALIFORNIA
INFORMATION RESOURCES DEPARTMENT
BERKELEY, CALIFORNIA 94720